Influence of Magnetic Field Structure on the Conduction Cooling of Flare Loops

by

S. K. Antiochos
P. A. Sturrock

March 1975

SUIPR Report No. 656

National Aeronautics and Space Administration Grant NGL 05-020-272, Office of Naval Research Contract N00014-75-C-0572

INSTITUTE FOR PLASMA RESEARCH
STANFORD UNIVERSITY, STANFORD, CALIFORNIA

INFLUENCE OF MAGNETIC FIELD STRUCTURE ON THE CONDUCTION COOLING OF FLARE LOOPS

by

S.K. Antiochos* and P.A. Sturrock

National Aeronautics and Space Administration
Grant NGL-05-020-272

Office of Naval Research
Contract N00014-75-C-0673,

SUIPR 656

Mar 76

21 p.

Institute for Plasma Research
Stanford University
Stanford, California

*Also Department of Applied Physics

I. Introduction

Observations in the soft x-ray part of the spectrum indicate that most flares produce a hot quasi-thermal plasma at coronal heights with maximum temperatures of order 3×10^7 K. The dominant cooling processes are believed to be radiation and conduction to the chromosphere (Culhane et al., 1970). Simple estimates based on a specific flare model (Sturrock, 1968) indicate that, in this temperature regime, conduction cooling is more important than radiation. This conclusion is supported by detailed calculations by Strauss and Papagiannis (1971) on the same flare model, and by data analysis carried out by Moore and Datlowe (1975) on 17 small flares.

If conduction is indeed the dominant cooling mechanism, then magnetic-field geometry will have a strong influence on the cooling rate. Optical observations (see, for instance, Fisher, 1971) show that the coronal post-flare plasma typically has a loop-like structure, presumably due to the influence of magnetic fields. Rust and Bar (1973) have deduced from their observations that the field in post-flare regions is well represented by a potential field, especially at large heights. In the case which they investigated (the flare of August 7, 1972), the field strength at the top of the loops was of order 50 gauss while that at the base of the loops was over 1000 gauss. This shows that there is a large change in cross section of a flux tube along its length, a factor which is not taken into account in calculations mentioned above.

It therefore seems desirable to study the evolution of a hot post-flare plasma confined to a flux tube which has substantial

variation of magnetic field strength along its length. We shall concern ourselves with the phase in which the plasma cools primarily by thermal conduction to the chromosphere. This is a substantial simplification of the real problem, which involves also radiation and mass motion. Nevertheless, we consider this study to be a useful first step in trying to understand the influence of magnetic-field geometry on the cooling of flare plasma.

II. Model

Since thermal conduction across magnetic-field lines is negligible in comparison with thermal conduction along field lines, we may consider the cooling of a small flux tube independently of all other flux tubes. We adopt the model shown in Figure 1, showing a symmetrical flux tube which extends a height H above the top of the chromosphere which is the base of our model. The independent variable s measures distance along the loop from the top of the loop. The variation of cross-sectional area is described by a function A(s), normalized to unity at the top of the loop.

More specifically, we assume the field to be current-free above the chromosphere and to be identical with the field produced either by a horizontal line dipole (L) or by a horizontal point dipole (P) at a depth D below the chromosphere. It is convenient to use the angle θ defined in Figure 1 in place of s as the independent variable. The relationship between s and θ is given by

$$\frac{s}{R} = \theta \qquad (2.1.1)$$

$$\frac{s}{R} = \frac{1}{2} \sin\theta \, (1+3\sin^2\theta)^{1/2} + \frac{1}{2} 3^{-1/2} \, \ell n[3^{1/2} \sin\theta + (1+3\sin^2\theta)^{1/2}] \quad (2.1.P)$$

where

$$R = H + D \quad , \qquad (2.2)$$

and we repeat equations for the line-dipole and point-dipole models, as necessary. The area function $A(\theta)$, normalized to unity at $\theta = 0$, is given by

$$A(\theta) = \cos^2\theta \qquad (2.3.L)$$

or

$$A(\theta) = \cos^6\theta \, (1 + 3\sin^2\theta)^{-1/2} \quad . \qquad (2.3.P)$$

For a plasma of temperature 10^7 K, the scale height is approximately the same as the solar radius. As a result, it is a reasonable approximation to ignore gravitational effects.

The key simplification in our model is to assume that each dependent variable may be expressed as a function of s multiplied by a function of t. In particular, we assume that the electron density n is expressible as

$$n = f(s) \, g(t) \quad . \qquad (2.4)$$

If, in addition, we assume that there is no exchange of plasma between the flux tube and the chromosphere, it follows that g = constant so that

$$n = n(s) \quad . \qquad (2.5)$$

It now follows from the equation of continuity that the plasma is static. Then, ignoring gravitational effects, it follows from the equation of

motion that the plasma must be isobaric, so that

$$p = p(t) \quad , \tag{2.6}$$

where p is the total plasma pressure. For a fully ionized hydrogen plasma, p and n are related by

$$p = 2nkT \quad . \tag{2.7}$$

Since heating and radiation losses are being neglected, the heat equation is simply

$$\frac{\partial}{\partial t}(3nkT) = \frac{1}{A}\frac{\partial}{\partial s}\left(AK\frac{\partial T}{\partial s}\right) \tag{2.8}$$

where K is the thermal conductivity. We adopt the Spitzer (1962) form

$$K = \alpha T^{5/2} \tag{2.9}$$

where, with accuracy sufficient for our needs, we may take $\alpha = 10^{-6}$.

On using equations (2.5), (2.6) and (2.7), we find that the heat equation may be rewritten in the following form,

$$\frac{3}{2}p^{-7/2}\frac{dp}{dt} = \frac{\alpha}{A}\frac{d}{ds}\left(A\frac{dG}{ds}\right) \tag{2.10}$$

where we have introduced the symbol

$$G(s) = \frac{2}{7}[2kn(s)]^{-7/2} \quad . \tag{2.11}$$

It is to be noted that terms on the left-hand side of equation (2.10) are functions only of t whereas terms on the right-hand side are functions only of s. Hence each side of the equation must be equal to a constant, which we take to be $-\frac{3}{5}\tau^{-1}p_0^{-5/2}$. With this choice, we find that p(t) is

expressible as

$$p(t) = p_0(1 + t/\tau)^{-2/5} \quad , \tag{2.12}$$

where $p = p_0$ at $t = 0$. For the two cases considered, we find that

$$G(\theta) = G_0 - \frac{3}{10}\,\alpha^{-1}\,R^2\,p_0^{-5/2}\,\tau^{-1}\,.\,\theta\tan\theta \tag{2.13.L}$$

or

$$G(\theta) = G_0 - \frac{3}{10}\,\alpha^{-1}\,R^2\,p_0^{-5/2}\,\tau^{-1}\,.\,\frac{\sin^2\theta}{\cos^4\theta}\,\gamma_1(\theta) \tag{2.13.P}$$

where

$$\gamma_1(\theta) = \frac{1}{70}\,(64 + 32\cos^2\theta - 11\cos^4\theta - 15\cos^6\theta) \quad . \tag{2.14}$$

Since $\gamma_1(\theta)$ is a slowly varying function of θ, confined to the range $0.91 < \gamma < 1.09$, we replace it by unity in subsequent formulas.

We denote by θ_b the value of θ at the "base" of the model identified with the chromosphere. This is related to the height of the loop and the depth of the dipole by

$$H = R\sin^2\theta_b \quad , \qquad D = R\cos^2\theta_b \tag{2.15.L}$$

or

$$H = R(1 - \cos^3\theta) \quad , \qquad D = R\cos^3\theta_b \quad . \tag{2.15.P}$$

On noting that $G(\theta_b) \approx 0$, we see from equations (2.13) that τ is expressible as

$$\tau = \tau_0\,\theta_b\tan\theta_b \tag{2.16.L}$$

or

$$\tau = \tau_0\tan^2\theta_b\sec^2\theta_b \quad , \tag{2.16.P}$$

where

$$\tau_0 = \frac{21}{20}\,\alpha^{-1}\,p_0\,T_{00}^{-7/2}\,R^2 \quad . \tag{2.17}$$

In this expression, $p_0 = p(0)$ and $T_{00} = T(0,0)$.

On using equations (2.7) through (2.17), we obtain the following expression for the temperature:

$$T(\theta,t) = T_0(t) \left\{1 - \frac{\cos\theta_b}{\theta_b \sin\theta_b} \frac{\theta \sin\theta}{\cos\theta}\right\}^{2/7} , \qquad (2.18.L)$$

or

$$T(\theta,t) = T_0(t) \left\{1 - \frac{\cos^4\theta_b}{\sin^2\theta_b} \frac{\sin^2\theta}{\cos^4\theta}\right\}^{2/7} , \qquad (2.18.P)$$

where $T_0(t)$, the temperature at the top of the loop, is given by

$$T(0,t) = T_0(t) = T_{00}(1 + t/\tau)^{-2/5} . \qquad (2.19)$$

From equations (2.9) and (2.18), we find that the heat flux is given by

$$F(\theta,t) = F_0(t) \frac{\cos\theta_b}{\theta_b \sin\theta_b} \cdot \frac{\theta + \sin\theta\cos\theta}{2\cos^2\theta} \qquad (2.20.L)$$

or

$$F(\theta,t) = F_0(t) \frac{\cos^4\theta_b}{\sin^2\theta_b} \cdot \frac{\sin\theta}{\cos^6\theta} \gamma_2(\theta) \qquad (2.20.P)$$

where

$$F_0(t) = \frac{4}{7} \alpha R^{-1} T_0^{7/2}(t) \qquad (2.21)$$

and

$$\gamma_2(\theta) = (1 + 3\sin^2\theta)^{1/2} (1 - \sin^2\theta + \frac{3}{5}\sin^4\theta - \frac{1}{7}\sin^6\theta) . \qquad (2.22)$$

It is found that $\gamma_2(\theta)$ also is a slowly varying function of θ, varying in the range $.91 < \gamma_2 < 1.05$. Hence in subsequent calculations we replace γ_2 by unity.

The heat flux $F_b(t)$ at the base of the tube is found to be

$$F_b(t) = F_0(t) \left\{ \frac{1}{2\theta_b} + \frac{1}{\sin(2\theta_b)} \right\} . \qquad (2.23.L)$$

or

$$F_b(t) = F_0(t) \cdot \frac{1}{\sin \theta_b \cos^2\theta_b} . \qquad (2.23.P)$$

The total energy loss rate, referred to unit cross-sectional area at the top of the tube, is given by

$$S = 2 A(\theta_b) F_b(t) \qquad (2.24)$$

which leads to the expression

$$S(\theta_b,t) = F_0(t) \left\{ \frac{\cos^2\theta_b}{\theta_b} + \cot \theta_b \right\} \qquad (2.25.L)$$

or

$$S(\theta_b,t) = 2F_0(t) \cos^3\theta_b \cot \theta_b (1 + 3 \sin^2\theta_b)^{-1/2} . \qquad (2.25.P)$$

III. Cooling Rate

In discussing results of our analysis of this model, it is convenient to introduce the symbol Γ for the "compression factor" defined either as the area ratio

$$\Gamma = \frac{1}{A_b} \qquad (3.1)$$

or as the magnetic field ratio

$$\Gamma = \frac{B(\theta_b)}{B(0)} . \qquad (3.2)$$

We see from equation (2.3) that Γ is related to θ_b by

$$\Gamma = \sec^2\theta_b \qquad (3.3.L)$$

or

$$\Gamma = \sec^6\theta_b \ (1 + 3 \sin^2\theta_b)^{1/2} \ . \qquad (3.3.P)$$

We may now compare the cooling time $\tau(\Gamma)$ of a loop structure with compression factor Γ to τ_p, the cooling time of a planar model with the same loop length s_b. Since τ_p is related to τ_0 by

$$\tau_p = \tau_0 \ (s_b/R)^2 \qquad (3.4)$$

we may calculate from equation (2.11) and (2.16) the dependence of $\tau(\Gamma)\tau_p$ on Γ, as shown in Figure 2. We note that the cooling time is a sensitive function of Γ. The analysis by Rust and Bar (1973) of the loops produced by the flares of August, 1972, show that, for those events, Γ took a range of values from 4 to 30. Such values clearly have an important effect in influencing heat loss.

The initial temperatures and densities of flare-produced soft x-ray-emitting regions are typically $T = 10^{7.5}$ K and $n \approx 10^{11}$ cm^{-3}, with $H \sim 10^{9.5}$ cm. On using equations (2.17) and (3.4), we find that $\tau_p \approx 10^2$ s. By comparison, the radiative cooling time may be estimated from

$$\tau_R = \frac{3}{2} \frac{p}{n^2 \Lambda(T)} \ , \qquad (3.5)$$

where $\Lambda(T)$ is the radiation loss function calculated by Cox and Tucker (1969). We find, for the proposed parameters, that $\tau_R \approx 10^{3.5}$ s. If the compression factor Γ is large enough, the conduction cooling time

may be increased by an order of magnitude to make it comparable with τ_R. In any case, radiation must eventually dominate since, as the plasma cools, τ_p increases as T decreases. Figure 2 indicates that radiation will dominate at a higher temperature in a loop structure with large compression factor than it would in a loop structure with small compression factor. The fact that the influence of the magnetic-field geometry is to increase the cooling time, by comparison with a planar model, implies that a larger fraction of the initial energy will be radiated. Since it is unlikely that Γ will exceed 10^2, it appears that the present model should be valid for the initial cooling phase of post-flare plasma loops.

IV. Heat Flux and Evaporation

Since the cooling rate decreases with increasing compression factor, it is clear that the total energy loss rate into the chromosphere must decrease as Γ increases. The ratio of the energy loss rate of a flare loop to that of a planar model is plotted against Γ in Figure 3, where we have used

$$F_p = F_0(t) \cdot R/s_b \quad , \tag{4.1}$$

for the heat flux in the planar model. We see that the energy loss by thermal conduction may be decreased by an order of magnitude or more by the influence of magnetic-field geometry.

The ratio of the heat flux of a loop model to that of a planar model is shown in Figure 4, from which we see that the heat flux (per unit area) is greater for a loop structure than for a planar structure. The magnetic field acts as a funnel increasing the heat

flux per unit area, but not rapidly enough to compensate for the decrease in area, so that the total energy loss by thermal conduction decreases as the compression factor increases.

Even in the case of a planar model, one faces the difficulty that the high heat flux into the chromosphere from a post-flare loop, of order 10^9 erg cm^{-2} s^{-1}, cannot be maintained in the chromosphere because the thermal conductivity there is too low. Such fluxes are also too high to be converted into chromospheric radiation. It seems most likely that the excess heat flux into the chromosphere results in evaporation of chromospheric material. Since the heat fluxes are even higher when the effect of magnetic-field geometry is taken into account, the likelihood of evaporation becomes greater. Evaporation will increase the density in the loop, thus leading to a higher rate of energy loss by radiation.

We recognize that a complete treatment of the evolution of flare plasma must take account of evaporation. We are developing the present model to include this process. This more general study will help to delineate the range of applicability of the present model, which ignores all plasma motion. Our present assessment is that evaporation will occur mainly at the initial stage in development of flare plasma, probably in response to bombardment of the chromosphere by a flux of high-energy particles. After the plasma is evaporated, there should be a second stage described approximately by the present model. After further cooling, radiation will become the dominant cooling mechanism and this represents a third stage which is the subject of another article being prepared for publication.

V. Discussion

The model developed in this article is believed to be relevant to the early decay phase of post-flare plasma. Although the model leads to a very simple form for the dependence of plasma temperature on time (equation (2.19)), it is unlikely that this law can be compared directly with soft x-ray observations from post-flare plasma, since such plasma will typically occupy flux tubes covering a wide range of height and the decay constant τ will vary from tube to tube. In order to test the model, observations of high spatial and temporal resolution are necessary so that both the temperature evolution and the geometry of a flare loop can be determined. Alternatively, it would be possible to consider the behavior of a model comprising a finite range of field lines and to integrate the total x-ray emission from this model. Such results might then be compared directly with observational data.

The main aim of this article was to investigate the influence upon flare cooling of realistic magnetic-field geometries. This is summarized by Figures 1 through 4, in which the important parameter characterizing the geometry is the "compression factor" Γ. We see that magnetic-field geometry can have a large effect on the flare behavior, indicating that it may be quite misleading to treat the evolution of flare plasma on the basis of a plane-parallel model.

Acknowledgements

One of us (P.A.S.) wishes to thank Professors G.R. Burbidge and L.E. Peterson and their colleagues at the University of California at San Diego for their kind hospitality in the spring of 1975, when this work was initiated. This work was supported by the National Aeronautics and Space Administration under grant NGL 05-020-272 and the Office of Naval Research under contract N00014-75-C-0673.

References

Cox, D.P. and Tucker, W.H. 1969, Ap. J. 157, 1157.

Culhane, J.L., Vesecky, J.F. and Phillips, K.J.H. 1970, Sol. Phys. 15, 394.

Fisher, R.R. 1971, Sol. Phys. 19, 440.

Moore, R.L. and Datlowe, D.W. 1975, Sol. Phys 43, 189.

Rust, D.M. and Bar, V. 1973, Sol. Phys. 33, 445.

Spitzer, L. 1962, "Physics of Fully Ionized Gases", (Wiley Interscience, New York).

Strauss, F.M. and Papagiannis, M.D. 1971, Ap. J. 164, 369.

Sturrock, P.A. 1968, Proc. I.A.U. Symp. No. 35, Structure and Evolution of Solar Active Regions (Dordrecht: Reidel Publishing Co.), p. 471.

Figure Captions

Figure 1: The geometry of our loop model. s is the distance along a field line measured from the top of the loop. A(s) is the cross-sectional area of the flux tube.

Figure 2: Ratio of cooling times for a loop and for a planar (constant cross-section) model as a function of Γ, the ratio of the field strength at the base of the loop to that at the top. The solid line refers to a point dipole and the broken line to a line dipole.

Figure 3: Ratio of energy loss rates for a loop and for a planar (constant cross-section) model as a function of Γ, the ratio of the field strength at the base of the loop to that at the top. The solid line refers to a point dipole and the broken line to a line dipole.

Figure 4: Ratio of base heat fluxes for a loop and for a planar (constant cross-section) model as a function of Γ, the ratio of the field strength at the base of the loop to that at the top. The solid line refers to a point dipole and the broken line to a line dipole.

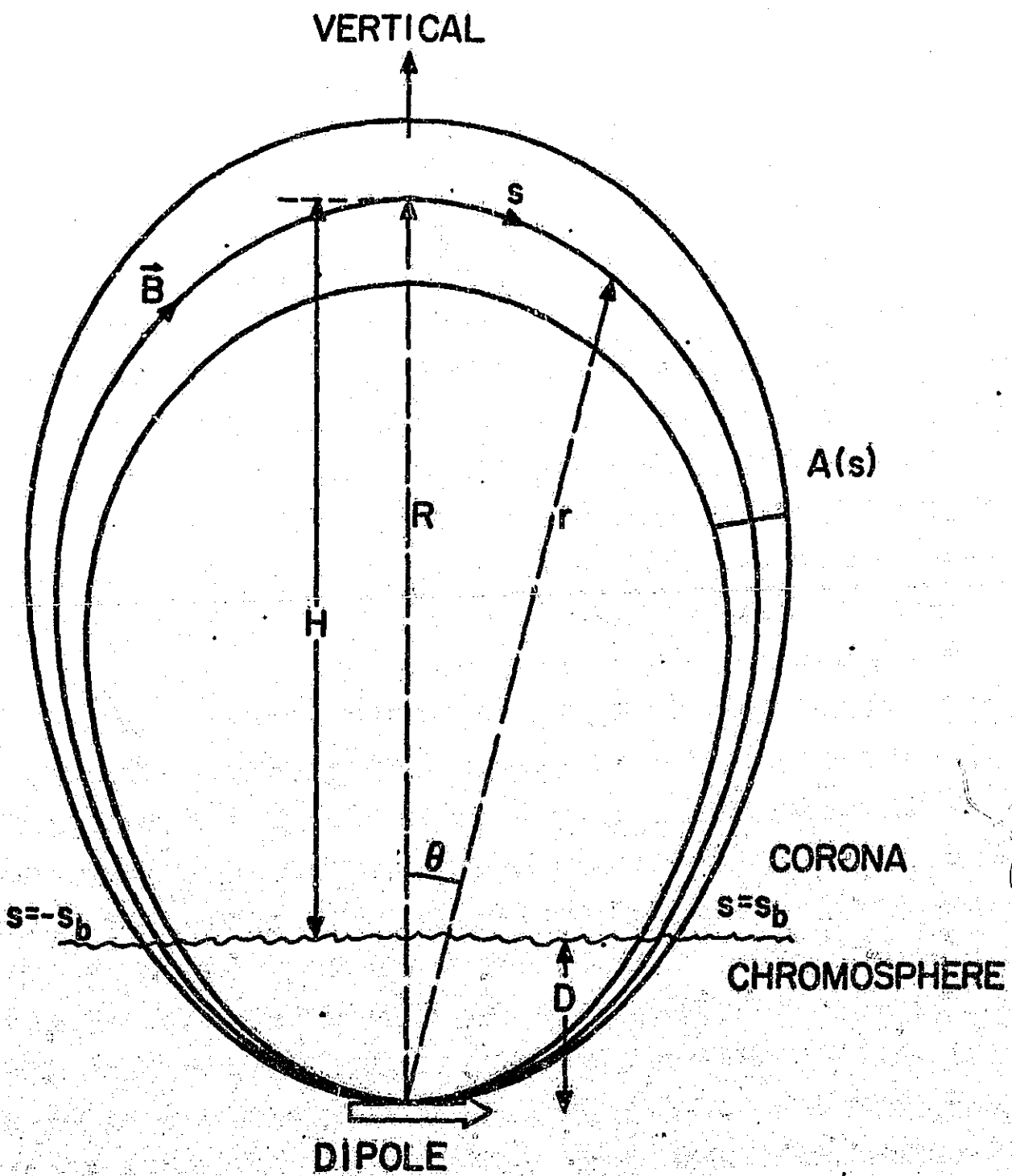
VERTICAL
s
$\vec{B}$
A(s)
R
r
H
θ
CORONA
s=-s_b
s=s_b
CHROMOSPHERE
D
DIPOLE

Figure 1

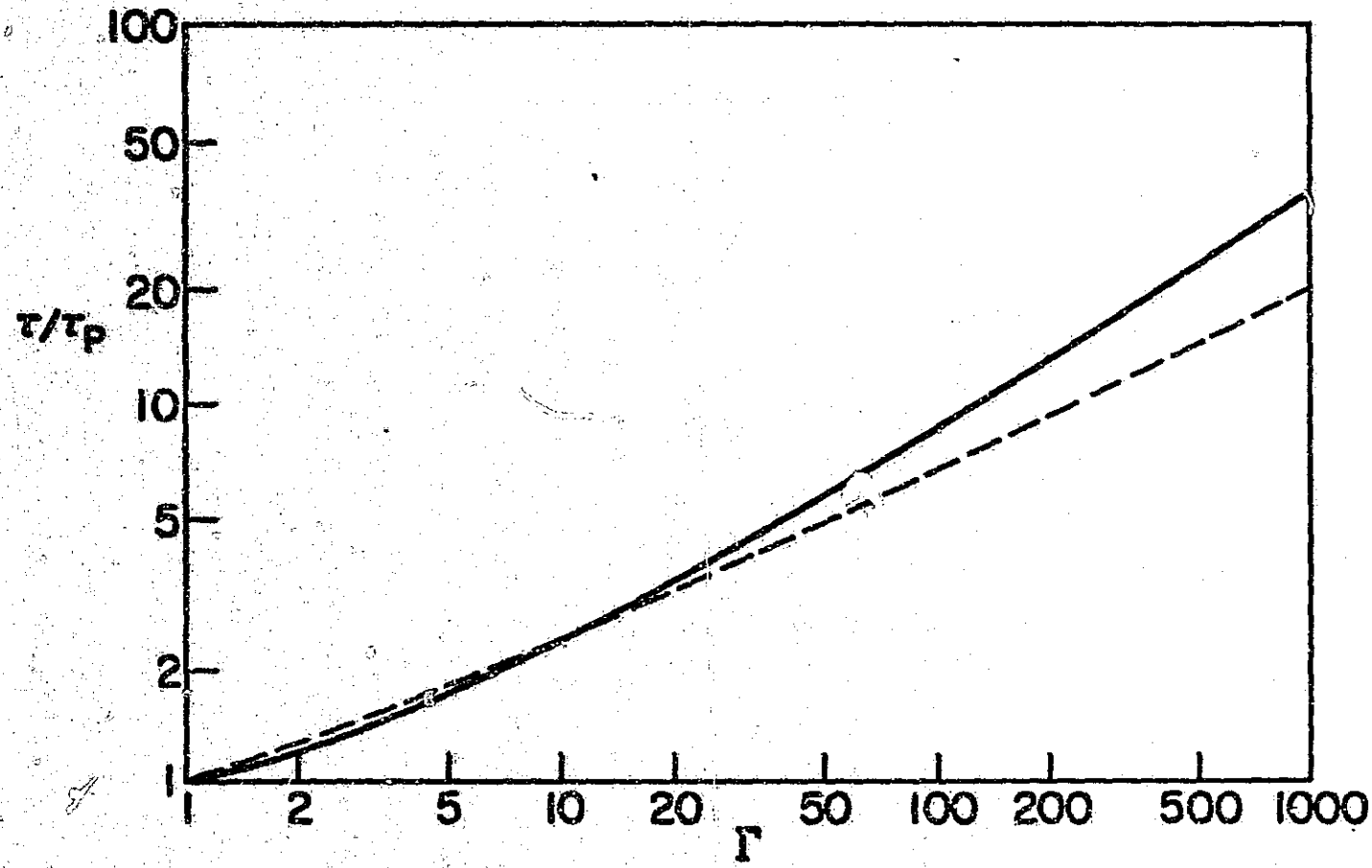

Figure 2

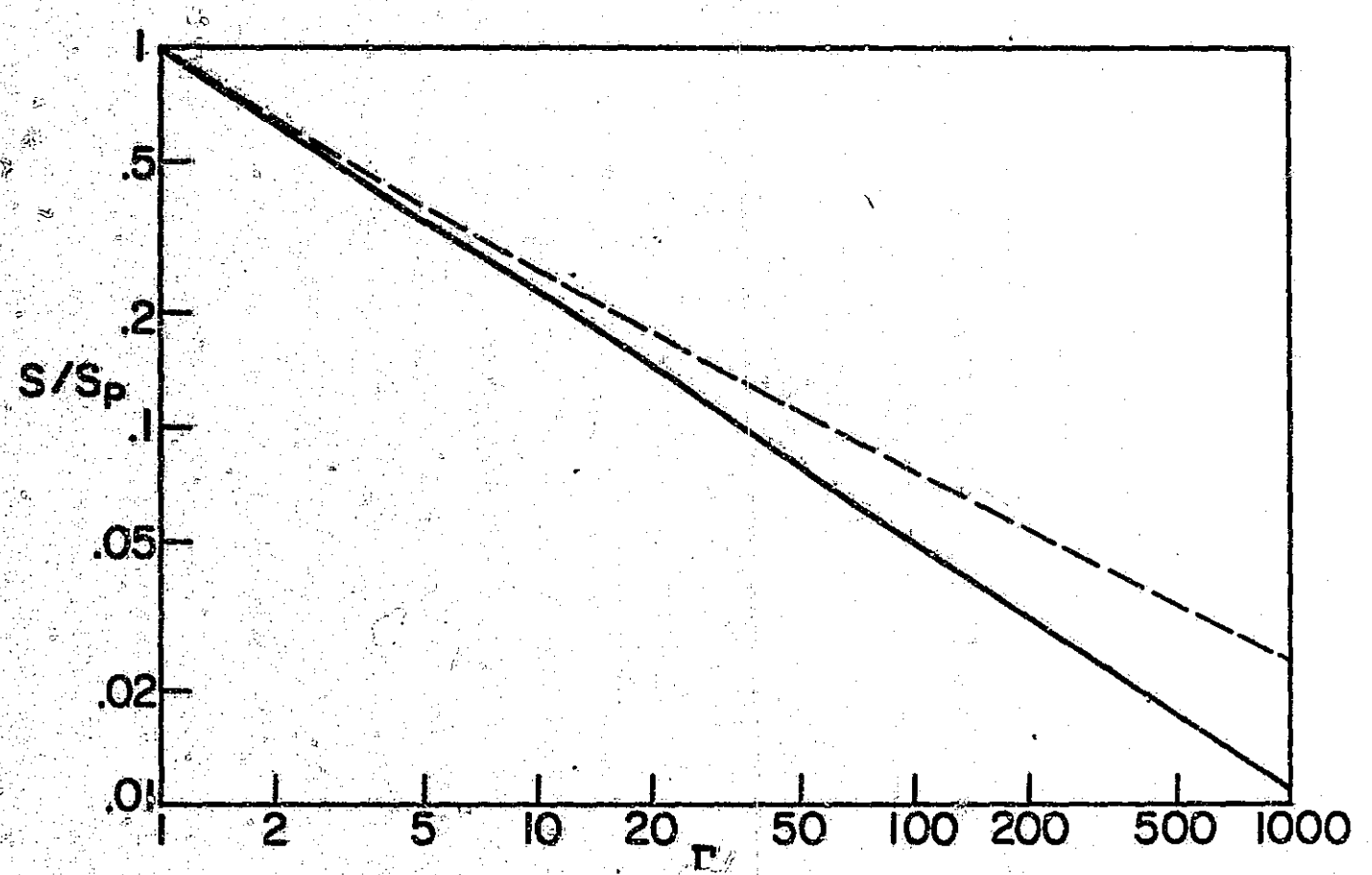

Figure 3

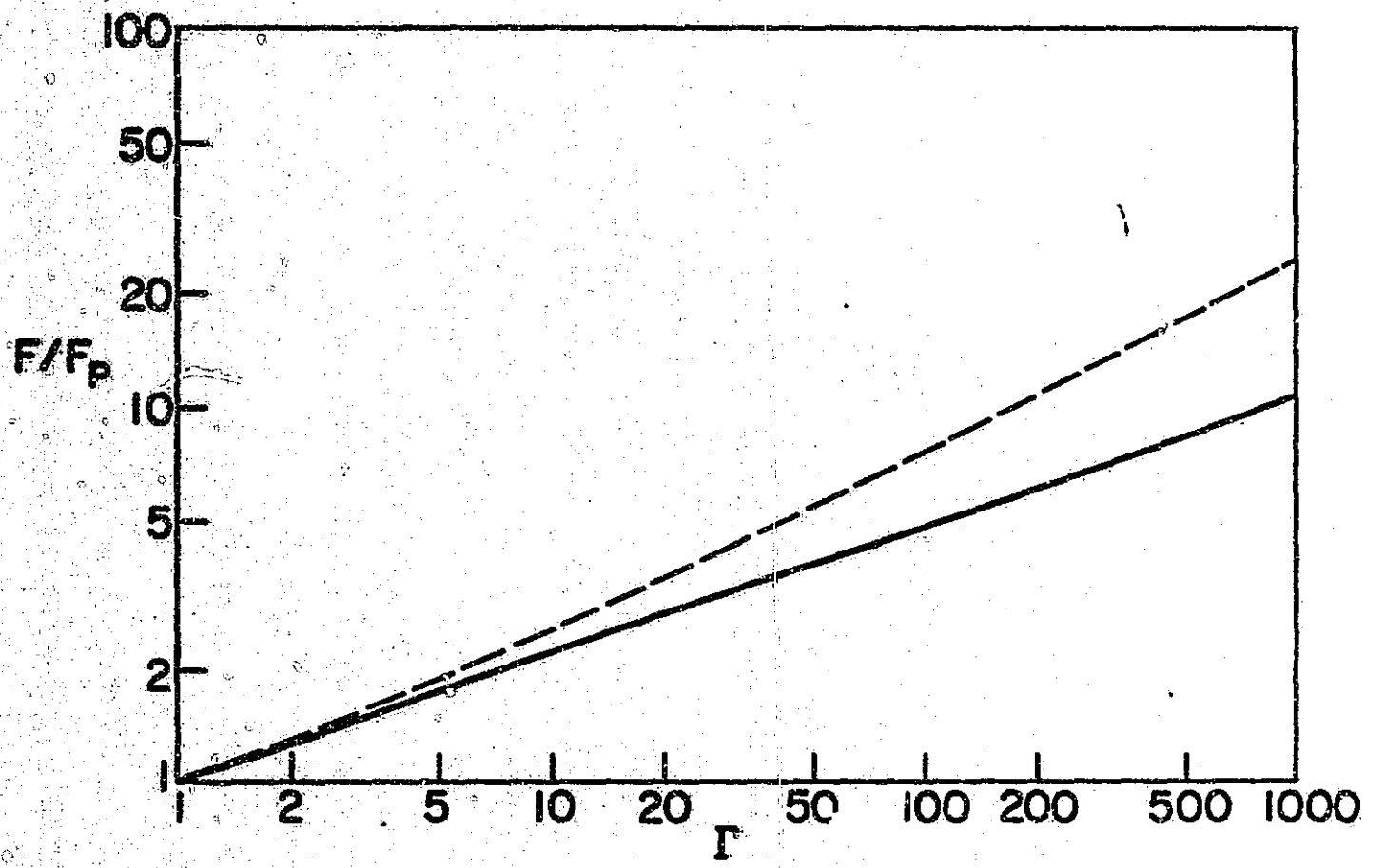

Figure 4